

Article

Treatment of Oily Wastewater by the Optimization of Fe₂O₃ Calcination Temperatures in Innovative Bio-Electron-Fenton Microbial Fuel Cells

Jung-Chen Wu ¹, Wei-Mon Yan ², Chin-Tsan Wang ^{3,*}, Chen-Hao Wang ^{1,*}, Yi-Hao Pai ⁴, Kai-Chin Wang ¹, Yan-Ming Chen ⁵, Tzu-Hsuan Lan ⁵ and Sangeetha Thangavel ²

¹ Department of Materials Science and Engineering, National Taiwan University of Science and Technology, No. 43, Keelung Rd., Sec. 4, Da'an Dist., Taipei 10607, Taiwan; shlayex@yahoo.com.tw (J.-C.W.); v1234eszxcv@gmail.com (K.-C.W.)

² Department of Energy and Refrigerating Air-Conditioning Engineering, National Taipei University of Technology, 1, Sec. 3, Zhongxiao E. Rd., Taipei 10608, Taiwan; wmyan1234@gmail.com (W.-M.Y.); geetha.vishnu@gmail.com (S.T.)

³ Department of Mechanical and Electro-Mechanical Engineering, National Ilan University, No. 1, Sec. 1, Shennong Rd., Yilan 26047, Taiwan

⁴ Department of Opto-Electronic Engineering, National Dong Hwa University, No. 1, Sec. 2, Da Hsueh Rd., Shoufeng, Hualien 97401, Taiwan; paiyihao@mail.ndhu.edu.tw

⁵ Department of Materials and Mineral Resources Engineering & Institute of Materials Science and Engineering National Taipei University of Technology, No. 1, Sec. 3, Zhong-Xiao E. Rd., Taipei 10608, Taiwan; ktotheo@hotmail.com (Y.-M.C.); jh2111900@hotmail.com (T.-H.L.)

* Correspondence: ctwang@niu.edu.tw (C.-T.W.); chwang@mail.ntust.edu.tw (C.-H.W.); Tel.: +886-3-935-7400 (ext. 7459) (C.-T.W.); +886-2-2730-3715 (C.-H.W.); Fax: +886-3-931-1326 (C.-T.W.); +886-2-2737-6544 (C.-H.W.)

Received: 20 January 2018; Accepted: 2 March 2018; Published: 6 March 2018

Abstract: Due to the fact that Iron oxide (Fe₂O₃) is known to have a good effect on the photochemical reaction of catalysts, an investigation in this study into the enhancement of the degradation performance of bio-electro-Fenton microbial fuel cells (Bio-E-Fenton MFCs) was carried out using three photocatalytic cathodes. These cathodes were produced at different calcination temperatures of Fe₂O₃ ranging from 500 °C to 900 °C for realizing their performance as photo catalysts within the cathodic chamber of an MFC, and they were compared for their ability to degrade oily wastewater. Results show that a suitable temperature for the calcination of iron oxide would have a significantly positive effect on the performance of Bio-E-Fenton MFCs. An optimal calcination temperature of 500 °C for Fe₂O₃ in the electrode material of the cathode was observed to produce a maximum power density of 52.5 mW/m² and a chemical oxygen demand (COD) degradation rate of oily wastewater (catholyte) of 99.3% within one hour of operation. These novel findings will be useful for the improvement of the performance and applications of Bio-E-Fenton MFCs and their future applications in the field of wastewater treatment.

Keywords: bio-electro-Fenton microbial fuel cells (Bio-E-Fenton MFCs); wastewater; photo catalyst; degradation; calcination; chemical oxygen demand (COD)

1. Introduction

The Bio-Electro-Fenton Microbial Fuel Cells (Bio-E-Fenton MFCs) is a new framework and has been operated extensively because of its simultaneous wastewater treatment and power generation capability. Significantly, the electro-Fenton reaction consists of iron ions (Fe²⁺) and hydrogen peroxide, and has become a useful technology for treating organic pollutants in wastewater [1–10] as hydroxyl radicals (•OH) are generated in abundance within the electro-Fenton reaction [11]. Considering the working principle of

Bio-E-Fenton MFCs, electrons and protons are produced at the anode as a result of the microbial oxidation of substrates. Then, electrons move towards the cathode through an external circuit pathway, whereas the protons directly penetrate through a membrane and arrive at the cathode simultaneously. Finally, a complete reaction of redox is attained with the aid of oxygen in the cathodic reduction reaction of Bio-E-Fenton MFCs [12]. Although the electro-Fenton reaction is very feasible and effective in treating organic pollutants in wastewater, the COD removal is incomplete [13,14]. A new electro-Fenton system with an Fe@Fe₂O₃/CNT oxygen-fed gas diffusion cathode was able to degrade rhodamine B (RhB) reaching 91.5% within 120 min at neutral pH [11]. The anode was a Pt sheet with a surface area of 2.0 cm² and it also served as a pseudo reference electrode. Cyclic voltammetry experiments were performed and a couple of well-defined peaks were observed at ~0.62 V, which were ascribed to the overall redox potentials of the Fe³⁺/Fe²⁺ couple. However, 74.1% and 60.1% of RhB was degraded on the Fe@Fe₂O₃/ACF and Fe@Fe₂O₃/graphite cathodes, respectively. Polyaniline (PANI)-Fe₂O₃ nanocomposite was used to successfully enhance the dye adsorption efficiency of acid violet 19 dye, as the dye concentration was increased from 20–80 mg/lit, and the percentage removal of dye decreased from 98.5–90% for the adsorbent at 10 gm/lit [15]. For another kind of photo catalytic material like MoS₂, Liu et al. [16] have indicated that a system with MoS₂-RGO composites has a better photo catalytic performance than using pure MoS₂. Here, the MoS₂-RGO composite with 0.5 wt % RGO achieved the highest methylene blue (MB) degradation rate of 99% within 60 min [16]. Nan Xu et al. [17] reported that the anode was carbon felt assisted with granular graphite to enhance the anodic power density. Anaerobic sludge collected from the Mangrove Wetland in Shenzhen was used as a biocatalyst in the anodic chamber. The system with E2 (17β-estrodial) in the catholyte enhanced the voltage output to 0.29 V and the E2 removal efficiency leveled off within 6 h, reaching 85.5%, 96.4%, 88.6%, and 75.6% with an external load of 50, 150, 500, and 1000 Ω, respectively, while the corresponding power density values were 3.47, 4.35, 3.01, and 2.41 W/m³ [17].

Nevertheless, facing the issue of the weak performance of MFCs, many kinds of electrode materials such as carbon nanotube/polyaniline carbon paper, CNT/PANI carbon paper, have been developed [18]. Results showed that a lower ohm loss and a better power performance with a maximum power density of 1574 mW/m² were executed by using the CNT/PANI electrode. A voltage of 1.18 V and current of 12.8 mA in MFCs were achieved by using CNT/PANI carbon paper [18]. But some research works regarding the development of non-precious metal catalysts can be implemented for an effective oxygen reduction reaction (ORR) and the enhancement of MFC performance. Vitamin B12 (py-B12/C) pyrolyzed and supported by carbon black can be utilized as the cathode catalyst in the solid phase MFCs [19]. Therefore, an innovative endeavor of employing calcination iron oxide (Fe₂O₃) as a photo catalyst combined with the Bio-E-Fenton system, while simultaneously generating power, has not been previously reported for the treatment of organic wastewater. Fenton's reagent could function well under acidic conditions and during the anodic oxidation and cathode aeration resulted in a pH increase, inhibiting the generation of •OH and decreasing the COD removal rate [20–22]. In the experiment, 10% diluted sulfuric acid was added to the cathode solution to obtain a pH value of 3.0 [23]. The experimental mechanism of Fe₂O₃/carbon felt (CF) photo catalyst bio-electro-Fenton degradation of oily wastewater is illustrated in Figure 1. The first step ① in the cathode reaction: $2\text{H}^+ + 2\text{e}^- + \text{O}_2 \rightarrow \text{H}_2\text{O}_2$ (1–1), resulted in H₂O₂ accumulation in the cathode chamber via the two-electron reduction of dissolved O₂ in the Bio-E-Fenton MFCs and then FeSO₄ powder was also added as a source of Fe²⁺: $2\text{H}^+ + \text{Fe} \rightarrow \text{Fe}^{2+} + \text{H}_2$ (1–2); the second step ② Fe₂O₃ photo catalyst was added in the cathode chamber and a 300 W halogen lamp was used for the photo excitation of Fe₂O₃ in order to produce more hydroxyl radicals; the third step ③ finally showed the bio-electro-Fenton reaction at the cathode, where the hydroxyl radicals played a vital role in the degradation of products according to the reaction: $\text{Fe}^{2+} + \text{H}_2\text{O}_2 \rightarrow \text{Fe}^{3+} + \bullet\text{OH} + \text{OH}^-$ (1–3). This was followed by the reduction of Fe³⁺ to Fe²⁺. This was a chain reaction where Fe³⁺ got reduced to Fe²⁺ and then Fe²⁺ was oxidized into Fe³⁺. This was a completely physical reaction which took place at the cathode and microbes had no role to play. In the conclusion, the Bio-E-Fenton MFCs was reported to be an effective system to treat organic wastewater, as well as bio-refractory pollutants [13].

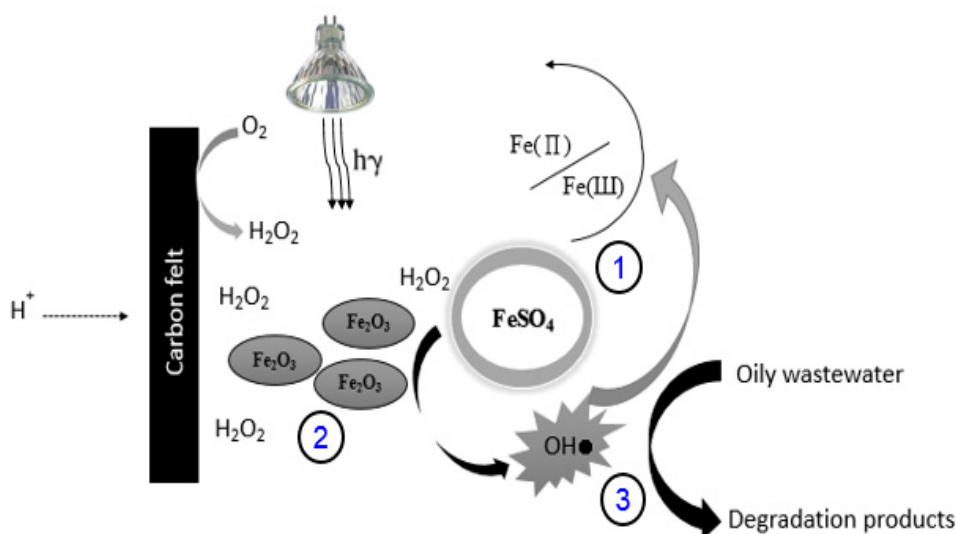


Figure 1. Proposed mechanism of Fe₂O₃/CF catalytic Bio-E-Fenton degradation of oily wastewater.

This research study has been carried out for gaining an in-depth understanding of the effects of calcination temperatures (500 °C to 900 °C) on the performance of Bio-E-Fenton MFCs. Based on the calcination temperature of Fe₂O₃, the photo catalyst structure will change and can be applied in this study for investigating the performance of MFCs. The results showed that the intensity of Fe₂O₃ will not vary greatly due to high calcination temperatures, but the crystalline particle size and surface morphology will be changed immensely [24]. This feature of Fe₂O₃ will enhance the COD removal efficiency of the MFC significantly [25–28]. Fe₂O₃/carbon felt (CF) has been selected to act as part of the cathode in Bio-E-Fenton MFCs because the photo catalysis of Fe₂O₃ can also produce hydroxyl radicals [11]. It can further combine with FeSO₄ to act as an iron source with H₂O₂ for producing more hydroxyl radicals (•OH), resulting in a higher degradation rate within a short time. In addition, a pH of 3 was maintained at the cathode chamber to treat refractory organic wastewater and this condition will not affect the pH of the anode chamber.

2. Experimental Design

2.1. Reactor Construction and Operation

An acrylic dual chambered tank with dimensions of 85 mm × 70 mm × 55 mm was selected for the construction of the Bio-E-Fenton MFC, as shown in Figure 2. Each chamber had a total volume of 200 mL with a proton exchange membrane Nafion-117 (80 mm × 70 mm) and carbon felt (CF, 60 mm × 60 mm × 5 mm) as the anode and cathode electrodes, respectively. The preparation method for the carbon felt is as follows: It was initially washed in hot H₂O₂ (10%, 90 °C) solution for 3 h to develop local Quinone sites on the carbon surface for improvement of the anode biocompatibility and increased quantity of anthraquinone [29]. In order to prevent the thermal heat transfer from the cathode to the anode, a Bakelite plate with dimensions of 100 mm × 50 mm × 20 mm (Figure 2) was employed in this study. Therefore, the power density would be influenced by the effect of the calcination temperature of Fe₂O₃ in the cathode chamber, but not by the temperature of the anode. In addition, a control reactor without Fe₂O₃ was not constructed and it was considered from the similar work of [30].

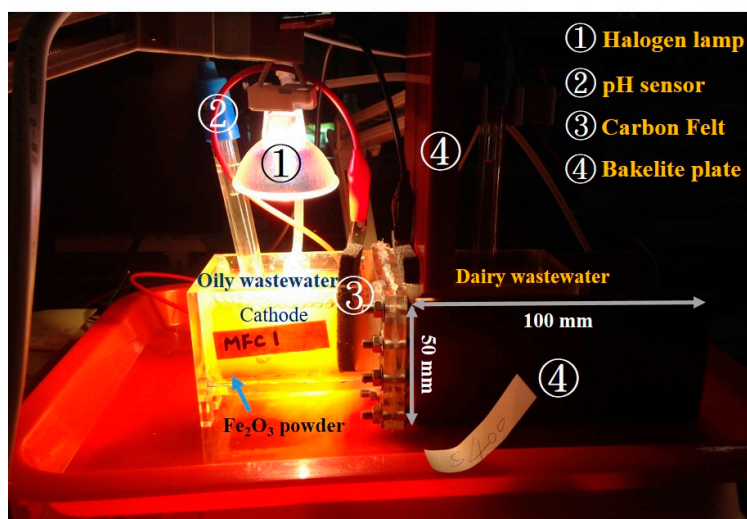


Figure 2. The experimental set-up of the proposed reactor.

2.2. Anolyte/Catholyte and Fe_2O_3 Catalyst Preparation

Kim et al. [31] proved that lactic acid wastewater can be employed to sustain the production of electrical energy in MFCs. Therefore, dairy wastewater was used in this study as the anolyte. During the early stage of fermentation of the dairy wastewater in the chamber, precipitate particulates were formed. Three layers were naturally formed when the wastewater was kept stagnant and were classified as top-level supernatant (clear fluid), a mid-level interface, and a bottom-level precipitate. Prior to the study, a conductivity experiment confirmed that the top-level supernatant in the chamber had the best conductivity of all, with an open-circuit voltage of 0.70 V, limiting current of 0.547 mA/m^2 , and an achievable maximum power density of 101.4 mW/m^2 . In addition, considering the fact that viscosity would influence microbial activity and also affect the power generation of MFCs [32], samples from the top-level supernatant were selected for further studies.

The water bodies [33] have long been contaminated by oil pollution [34–36], so artificially prepared oily wastewater was used as the catholyte in this study. A total of 1 mL of diesel was added to 1 L of water and heated in a magnetic heater and blended with a blender for 1 day at $50 \text{ }^\circ\text{C}$. As diesel was immiscible in water, 10 g of emulsifying (Tween 80) agent was added to aid the dissolution of the diesel in water. Molognoni et al. [37] assessed the bio-electrochemical treatability of industrial (dairy) wastewater by MFCs, and an MFC was built and continuously operated for 72 days, during which time the anodic chamber was fed with dairy wastewater and the cathodic chamber with an aerated mineral solution. The study demonstrated that industrial effluents from agrifood facilities can be treated by bio-electrochemical systems (BESs) with >85% (average) organic matter removal. The study by Marashi and Kariminia [38] proved that the wastewater concentration had an influence on the MFC performance and using the raw wastewater with the concentration of $8000 \text{ mg COD L}^{-1}$ resulted in the highest power density (65.6 mW m^{-2}) production. Kim et al. [39] reported that the MFC–Anaerobic fluidized membrane bioreactors (AFMBRs) achieved $89 \pm 3\%$ removal of the COD with an effluent of $36 \pm 6 \text{ mg-COD/L}$ over 112 days of operation.

A total of 270 mg of $FeCl_3$ (98%, Acros, Taipei, Taiwan) was dissolved in 30 mL of deionized water, and then 1 M of NaOH (98%, Fisher, Hampton, VA, USA) 1 mL and 0.5 M oxalic acid (98%, Acros) 750 μL were added to the Teflon tank, and the microwave was set up at $160 \text{ }^\circ\text{C}$ for 30 min. After that, the Fe_2O_3 sample solution was filtered through a membrane filter with a pore size of $0.2 \text{ } \mu\text{m}$ (Advantec, Toyo, Japan) and mixed with the $80 \text{ }^\circ\text{C}$ deionized water and Fe_2O_3 powder (by freeze-drying at $-50 \text{ }^\circ\text{C}$) under a vacuum for 5 h. Calcination of Fe_2O_3 was achieved by loading it into a fused aluminum oxide boat and the temperatures were set to $500 \text{ }^\circ\text{C}$, $700 \text{ }^\circ\text{C}$, and $900 \text{ }^\circ\text{C}$ for 30 min per/sample in a high temperature furnace. Following the calcination, the furnace was cooled to room temperature by natural convection.

2.3. Experimental Analysis

Electrochemical analysis was performed by the workstation (Jiehan ECW-5600, Taipei, Taiwan) to measure the polarization performance of the Bio-E-Fenton MFCs. For COD analysis, an instrument (SUNTEX-V2000 photometer, Taipei, Taiwan) was utilized with solutions diluted till $100\times$ with deionized water. The temperature for the calcination of Fe_2O_3 ($500\text{ }^\circ\text{C}$ – $900\text{ }^\circ\text{C}$) was applied using high temperature furnaces (Riki JH-2, Taipei, Taiwan). The pH was measured in the anode/cathode chambers by using a pH meter (SUNTEX SP-2300, Taipei, Taiwan) and dissolved oxygen (DO) by using the DO analyzer (CLEAN DO-200, Taipei, Taiwan). For material analysis, instruments like an X-ray diffractometer (Bruker D2 Phaser), field emission scanning electron microscope (FE-SEM) (JSM-6500F), and Field Emission Gun Transmission Electron Microscopy, FEG-TEM (FEI Tecnai™ G2 F-20 S-TWIN), were used.

3. Results and Discussions

3.1. Performance of the Fe_2O_3 - $500\text{ }^\circ\text{C}$ /CF in Bio-E-Fenton MFCs Power Generation

Polarization curves for the Bio-E-Fenton MFCs using Fe_2O_3 calcination from $500\text{ }^\circ\text{C}$ – $900\text{ }^\circ\text{C}$ are portrayed in Figure 3. The conditions adopted for the polarization test were listed as follows; two-electrode measurement, anode electrode connected (by copper wire) to the working electrode (WE); reference electrode 2 (RE2) was in the dairy wastewater solution; the cathode electrode was connected (by copper wire) to the counter electrode (CE) and reference electrode 1 (RE1) in oily wastewater solution. Here, the carbon felt ($60\text{ mm} \times 60\text{ mm} \times 5\text{ mm}$) was selected as the electrode and can be used to calculate the power density (power/working area of electrode) and current density (current/working area of electrode). It was clear that Fe_2O_3 - $500\text{ }^\circ\text{C}$ /CF produced an open circuit voltage of 0.55 V , a maximum current density of 349 mA/m^2 , and a maximum power density of 52.5 mW/m^2 , which was 2.6 fold higher compared to Fe_2O_3 - $900\text{ }^\circ\text{C}$. A comparison between previous studies of Bio-E-Fenton MFCs and this study has been made and the results are shown in Table 1. In addition, an original report related to TiO_2 has been addressed for showing its optoelectronic ability to generate hydrogen in water [40]. Table 2 shows the list of related cases of photo catalysts.

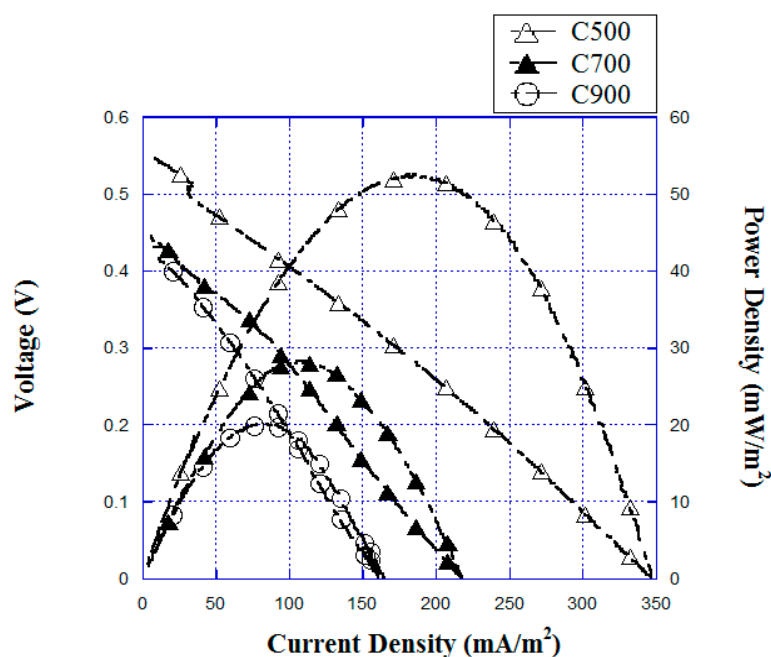


Figure 3. Polarization and power density curves of BEF-MFC at different calcination temperatures of Fe_2O_3 .

Table 1. Research studies using Bio-E-Fenton systems.

Power Density (mW/m ²)	COD Removal (%/h)	Ref.
430	78/1080	[13]
625	88/48	[14]
52.5	99.3/1	This study

Table 2. Different kinds of photo catalyst systems employed.

Material	Wavelength (nm)	COD Removal (%/min)	pH	Ref.
Fe@Fe ₂ O ₃ /CNT	555	91.5/120	8	[11]
PANI-Fe ₂ O ₃	545	98.5/90	8	[15]
MoS ₂ -RGO	450	99.0/60	7	[16]
Fe ₂ O ₃ -C500 °C/CF	410	99.3/60	3	This study

In consideration of the COD degradation rate, the Fe₂O₃-500 °C/CF performed better with 99.3% removal in 1 h and with an effluent concentration of 152 ± 5 mg-COD/mL/1 day. Generally speaking, a higher COD degradation rate was observed in this study compared to the other studies involving general bio-electro-Fenton systems [41] for the treatment of oily wastewater, with an efficiency that was 1.4 times higher (Table 3). The pH and DO at 700 °C were lower than those at 500 °C and 900 °C because under the constant resistance (1 K Ω) discharge at 700 °C, the DO and pH values affected the voltage output recorded from the long-term measurement. Nevertheless, the results of Table 3 indicated that a better power performance of the system and COD removal rate in the cathode chamber were observed at a calcination temperature of Fe₂O₃-500 °C, as it had a suitable pH and DO for befitting the biocompatibility [42–44] and electrical conductivity [45,46] in the system. The results showed that the maximum power density was 52.5 mW/m² and it was influenced by the calcination temperature of Fe₂O₃, which obviously showed that the power density decreased with increasing calcination temperature. In addition, the average temperature of the anode chamber was controlled at about 35–45 °C (by Bakelite plate) and the cathode temperature was higher than 70 °C (Shown in Table 3), which would be the effect of evaporation. Therefore, the measurement time was one hour and the time interval was based on the experimental reliability and neglecting the effect of evaporation in the cathode chamber.

Table 3. Performance of system @ calcination conditions of Fe₂O₃.

Parameter	500 °C	700 °C	900 °C	BF [30]
COD removal (%) @cathode	99.3	83.2	75.2	74.0
DO (ppm) @cathode	4.13	2.82	3.59	2.44
pH _{average}	2.1	1.8	2.4	3.0
PD _{max} (mW/m ²)	52.5	28.1	20.1	26.0
Temp. average/°C anode	34.6	43.7	42.7	22.6
Temp. average/°C cathode	71.6	74.9	72.7	24.1

BF: Bio-electro-Fenton system [30].

To further understand the impact of Fe₂O₃-C500-/CF on the degradation rate, the following three reasons were formulated: (1) the in situ reaction between Fe²⁺ leached from Fe₂O₃/FeSO₄ and H₂O₂ generated from the CF was kinetically more favorable than the reaction between H₂O₂ from the CF and Fe²⁺ in the bulk solution; (2) the calcination of Fe₂O₃ resulted in the formation of different crystal structures that affected the COD removal efficiency [47]; and (3) the photo catalyst accelerated chemical reactions [48] so that the strong oxidation of the hydroxyl radicals could quickly break the covalent bonds of diesel and enhance the degradation of wastewater [49].

3.2. Characterizations of the Calcinated Fe₂O₃

Figure 4 displays XRD patterns of the calcinated Fe₂O₃. The characteristic peaks of 500 °C Fe₂O₃ were at 24.2°, 33.3°, 35.6°, 40.9°, 49.6°, 54.2°, 62.6°, and 64.2°, corresponding to facet indexes of (012), (104), (110), (113), (024), (116), (214), and (300), respectively. The diffraction peaks at a 2θ value of 35.6° were ascribed to the (110) reflection of Fe₂O₃ [11]. Fe₂O₃ crystallographic structures can be controlled by varying their calcination temperatures. At a high calcination temperature, the intensity did not vary greatly, but the crystalline particle size and surface morphology changed immensely [24].

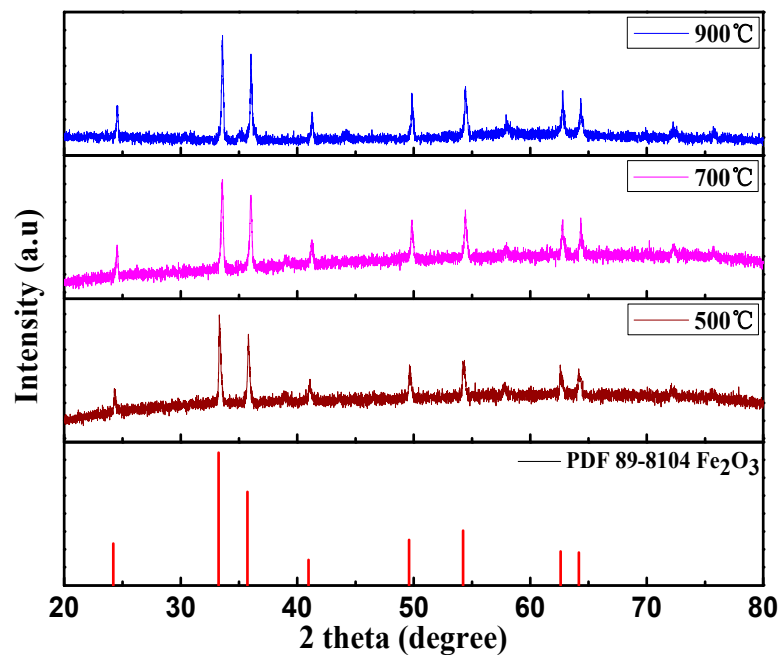


Figure 4. XRD patterns of Fe₂O₃ at different temperatures.

3.3. The Morphologies of the Fe₂O₃ at Different Calcination Temperatures

For analyzing the surface morphology of Fe₂O₃ at different temperatures, field emission scanning electron microscopy was used (Figure 5a–c). The Fe₂O₃ had an average particle size of 581 nm at 500 °C, 984 nm at 700 °C, and 1255 nm at 900 °C. Fe₂O₃ at 500 °C showed a layered stacked morphology and the particles were uniformly distributed with a large surface area. This showed that Fe₂O₃-C at 500 °C was better in terms of surface modification [50–52], which resulted in a maximum power density of 52.5 mW/m². In addition, the surface modification of Fe₂O₃ was indeed the main reason behind its best performance compared to the other systems.

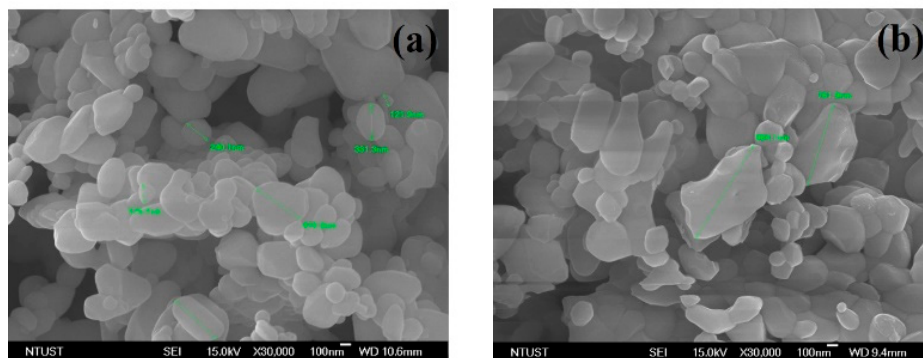


Figure 5. Cont.

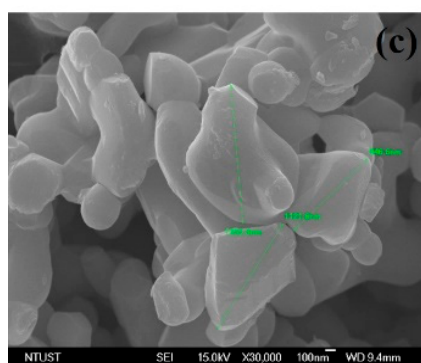


Figure 5. FE-SEM images of Fe_2O_3 at different calcination temperatures (a) 500 °C (b) 700 °C (c) 900 °C.

The TEM images depicted that highly-agglomerated Fe_2O_3 with a uniform size of ~ 28 nm in diameter affected the material structure of Fe_2O_3 after the calcination processes, as shown in Figure 6a, b. It should be noted that the structures after calcination at 500 °C to 700 °C led to a greater particle size and the lattice plane spacing of 0.21 to 0.26 nm. As shown in Figure 6c, calcination at 900 °C resulted in sheet-like structures and lattice plane spacing of 0.27 nm. The selected area diffraction pattern (SADP) showed excellent crystalline structure formations at 500 °C, which improved the COD degradation efficiency [25–28]. In addition, $\text{Fe}_2\text{O}_3\text{-C}500$ °C/CF had a better degradation rate of 99.3% in 1 h. This was a novel attempt where the $\text{Fe}_2\text{O}_3\text{-C}500$ °C/CF was combined with the bio-electro-Fenton reagent in MFCs.

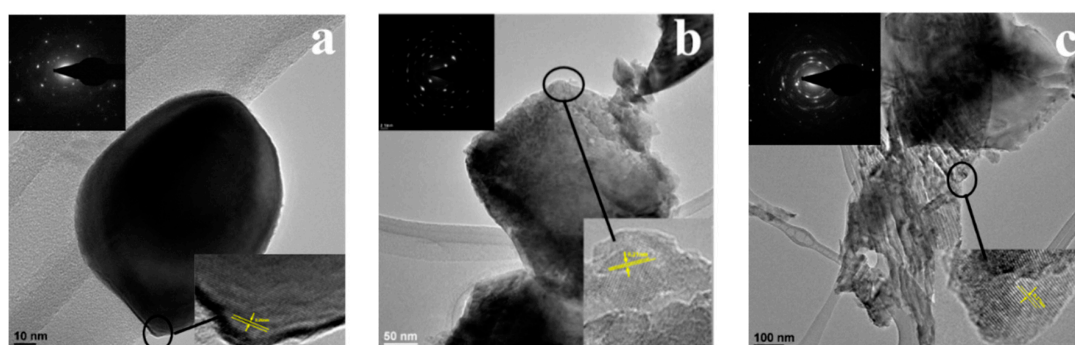


Figure 6. TEM images of Fe_2O_3 at different calcination temperatures (a) 500 °C (b) 700 °C (c) 900 °C.

4. Conclusions

In this study, the photo catalytic ability of iron oxide (Fe_2O_3) was investigated at different calcination temperatures ranging from 500 °C to 900 °C in a Bio-E-Fenton MFC for evaluating its effect on the degradation of dairy and oily wastewaters and power generation. A series of studies were executed and useful findings were addressed as follows: For the study of Fe_2O_3 in Bio-E-Fenton MFCs, firstly, the calcination at 500 °C brought about a better output voltage than in the case of the calcination at 900 °C, and its power density was also 2.6 times higher than at 900 °C. In addition, the COD degradation efficiency showed that $\text{Fe}_2\text{O}_3\text{-C}$ at 500 °C/CF had a better performance of 99.3% removal in 1 h and with an effluent of (152 ± 5 mg-COD/mL/1 day) operation, which was 1.3 times higher than the $\text{Fe}_2\text{O}_3\text{-C}$ at 900 °C/CF. Further, these evidences proved that calcination temperatures of 500 °C with 52.5 mW/m² would be optimal for Fe_2O_3 in Bio-E-Fenton MFCs because of its morphology with a uniform particle size and a larger surface area. In contrast, the degradation performance of 80.1% in 1 h was obtained by combining $\text{Fe}_2\text{O}_3\text{-C}500$ °C/CF with a bio-electro-Fenton reagent under non-illuminated conditions. Last but not the least, this innovative process was very promising for the treatment of organic wastewater treatment and the improved performance of related bio-electrochemical systems in the future.

Acknowledgments: The authors would like to acknowledge the generous funding support from MOST Taiwan under contract #MOST-104-2622-E-197-003-CC3, MOST-103-2221-E-197-022-MY3 and MOST-104-2628-E-011-003-MY3.

Author Contributions: Jung-Chen Wu: Operation of experiments, analysis and writing of article; Wei-Mon Yan: Support of experiments and integrated system; Chin-Tsan Wang: Guidance of experiments and modification of manuscript and reply of comments; Chen-Hao Wang: Guidance of chemical experiments; Yi-Hao Pai: Support and assistance of photo-catalyst; Kai-Chin Wang: Assistance of analysis in chemical part; Yan-Ming Chen: Assistance of analysis in material part; Tzu-Hsuan Lan: Assistance of analysis in material part; Sangeetha Thangavel: English modification of manuscript.

Conflicts of Interest: The authors declare no conflict of interest.

References

1. Khoufi, S.; Aloui, F.; Sayadi, S. Treatment of olive oil mill wastewater by combined process electro-Fenton reaction and anaerobic digestion. *Water Res.* **2006**, *40*, 2007–2016. [[CrossRef](#)] [[PubMed](#)]
2. Brillas, E.; Casado, J. Aniline degradation by Electro-Fenton[®] and peroxi-coagulation processes using a flow reactor for wastewater treatment. *Chemosphere* **2002**, *47*, 241–248. [[CrossRef](#)]
3. Liu, H.; Wang, C.; Li, X.; Xuan, X.; Jiang, C.; Cui, H.N. A novel electro-Fenton process for water treatment: Reaction-controlled pH adjustment and performance assessment. *Environ. Sci. Technol.* **2007**, *41*, 2937–2942. [[CrossRef](#)] [[PubMed](#)]
4. Panizza, M.; Oturan, M.A. Degradation of Alizarin Red by electro-Fenton process using a graphite-felt cathode. *Electrochim. Acta* **2011**, *56*, 7084–7087. [[CrossRef](#)]
5. Wang, A.; Qu, J.; Ru, J.; Liu, H.; Ge, J. Mineralization of an azo dye Acid Red 14 by electro-Fenton's reagent using an activated carbon fiber cathode. *Dyes Pigment.* **2005**, *65*, 227–233. [[CrossRef](#)]
6. Luo, M.; Yuan, S.; Tong, M.; Liao, P.; Xie, W.; Xu, X. An integrated catalyst of Pd supported on magnetic Fe₃O₄ nanoparticles: Simultaneous production of H₂O₂ and Fe²⁺ for efficient electro-Fenton degradation of organic contaminants. *Water Res.* **2014**, *48*, 190–199. [[CrossRef](#)] [[PubMed](#)]
7. Nidheesh, P.; Gandhimathi, R. Trends in electro-Fenton process for water and wastewater treatment: An overview. *Desalination* **2012**, *299*, 1–15. [[CrossRef](#)]
8. Nidheesh, P.; Gandhimathi, R.; Velmathi, S.; Sanjini, N. Magnetite as a heterogeneous electro Fenton catalyst for the removal of Rhodamine B from aqueous solution. *RSC Adv.* **2014**, *4*, 5698–5708. [[CrossRef](#)]
9. Ghoneim, M.M.; El-Desoky, H.S.; Zidan, N.M. Electro-Fenton oxidation of Sunset Yellow FCF azo-dye in aqueous solutions. *Desalination* **2011**, *274*, 22–30. [[CrossRef](#)]
10. Babuponnusami, A.; Muthukumar, K. A review on Fenton and improvements to the Fenton process for wastewater treatment. *J. Environ. Chem. Eng.* **2014**, *2*, 557–572. [[CrossRef](#)]
11. Ai, Z.; Mei, T.; Liu, J.; Li, J.; Jia, F.; Zhang, L.; Qiu, J. Fe@Fe₂O₃ core-shell nanowires as an iron reagent. 3. Their combination with CNTs as an effective oxygen-fed gas diffusion electrode in a neutral electro-Fenton system. *J. Phys. Chem. C* **2007**, *111*, 14799–14803. [[CrossRef](#)]
12. Zhuang, L.; Zhou, S.; Li, Y.; Liu, T.; Huang, D. In situ Fenton-enhanced cathodic reaction for sustainable increased electricity generation in microbial fuel cells. *J. Power Sources* **2010**, *195*, 1379–1382. [[CrossRef](#)]
13. Li, Y.; Lu, A.; Ding, H.; Wang, X.; Wang, C.; Zeng, C.; Yan, Y. Microbial fuel cells using natural pyrrhotite as the cathodic heterogeneous Fenton catalyst towards the degradation of biorefractory organics in landfill leachate. *Electrochem. Commun.* **2010**, *12*, 944–947. [[CrossRef](#)]
14. Wang, Y.; Feng, C.; Li, Y.; Gao, J.; Yu, C.-P. Enhancement of emerging contaminants removal using Fenton reaction driven by H₂O₂-producing microbial fuel cells. *Chem. Eng. J.* **2017**, *307*, 679–686. [[CrossRef](#)]
15. Patil, M.R.; Shrivastava, V.S. Adsorption removal of carcinogenic acid violet19 dye from aqueous solution by polyaniline-Fe₂O₃ magnetic nano-composite. *J. Mater. Environ. Sci* **2015**, *6*, 11–21.
16. Li, J.; Liu, X.; Pan, L.; Qin, W.; Chen, T.; Sun, Z. MoS₂-reduced graphene oxide composites synthesized via a microwave-assisted method for visible-light photocatalytic degradation of methylene blue. *RSC Adv.* **2014**, *4*, 9647–9651. [[CrossRef](#)]
17. Xu, N.; Zeng, Y.; Li, J.; Zhang, Y.; Sun, W. Removal of 17β-estrodial in a bio-electro-Fenton system: Contribution of oxidation and generation of hydroxyl radicals with the Fenton reaction and carbon felt cathode. *RSC Adv.* **2015**, *5*, 56832–56840. [[CrossRef](#)]
18. Wang, C.-T.; Huang, R.-Y.; Lee, Y.-C.; Zhang, C.-D. Electrode material of carbon nanotube/polyaniline carbon paper applied in microbial fuel cells. *J. Clean Energy Technol.* **2013**, *1*, 206–210. [[CrossRef](#)]

19. Wang, C.-H.; Wang, C.-T.; Huang, H.-C.; Chang, S.-T.; Liao, F.-Y. High stability pyrolyzed vitamin B12 as a non-precious metal catalyst of oxygen reduction reaction in microbial fuel cells. *RSC Adv.* **2013**, *3*, 15375–15381. [[CrossRef](#)]
20. Xu, N.; Zhou, S.; Yuan, Y.; Qin, H.; Zheng, Y.; Shu, C. Coupling of anodic biooxidation and cathodic bioelectro-Fenton for enhanced swine wastewater treatment. *Bioresour. Technol.* **2011**, *102*, 7777–7783. [[CrossRef](#)] [[PubMed](#)]
21. Fenton, H.J.H. LXXIII.—Oxidation of tartaric acid in presence of iron. *J. Chem. Soc. Trans.* **1894**, *65*, 899–910. [[CrossRef](#)]
22. Anotai, J.; Chen, C.-M.; Bellotindos, L.M.; Lu, M.-C. Treatment of TFT-LCD wastewater containing ethanolamine by fluidized-bed Fenton technology. *Bioresour. Technol.* **2012**, *113*, 272–275. [[CrossRef](#)] [[PubMed](#)]
23. Zhu, X.; Ni, J. Simultaneous processes of electricity generation and *p*-nitrophenol degradation in a microbial fuel cell. *Electrochem. Commun.* **2009**, *11*, 274–277. [[CrossRef](#)]
24. Fay, S.; Kroll, U.; Bucher, C.; Vallat-Sauvain, E.; Shah, A. Low pressure chemical vapour deposition of ZnO layers for thin-film solar cells: Temperature-induced morphological changes. *Sol. Energy Mater. Sol. Cells* **2005**, *86*, 385–397. [[CrossRef](#)]
25. Tian, C.; Zhang, Q.; Wu, A.; Jiang, M.; Liang, Z.; Jiang, B.; Fu, H. Cost-effective large-scale synthesis of ZnO photocatalyst with excellent performance for dye photodegradation. *Chem. Commun.* **2012**, *48*, 2858–2860. [[CrossRef](#)] [[PubMed](#)]
26. Yu, C.; Cao, F.; Li, X.; Li, G.; Xie, Y.; Jimmy, C.Y.; Shu, Q.; Fan, Q.; Chen, J. Hydrothermal synthesis and characterization of novel PbWO₄ microspheres with hierarchical nanostructures and enhanced photocatalytic performance in dye degradation. *Chem. Eng. J.* **2013**, *219*, 86–95. [[CrossRef](#)]
27. Zhou, W.; Sun, F.; Pan, K.; Tian, G.; Jiang, B.; Ren, Z.; Tian, C.; Fu, H. Well-Ordered Large-Pore Mesoporous Anatase TiO₂ with Remarkably High Thermal Stability and Improved Crystallinity: Preparation, Characterization, and Photocatalytic Performance. *Adv. Funct. Mater.* **2011**, *21*, 1922–1930. [[CrossRef](#)]
28. Xiong, J.; Cheng, G.; Li, G.; Qin, F.; Chen, R. Well-crystallized square-like 2D BiOCl nanoplates: Mannitol-assisted hydrothermal synthesis and improved visible-light-driven photocatalytic performance. *RSC Adv.* **2011**, *1*, 1542–1553. [[CrossRef](#)]
29. Feng, C.-H.; Li, F.-B.; Mai, H.-J.; Li, X.-Z. Bio-electro-Fenton process driven by microbial fuel cell for wastewater treatment. *Environ. Sci. Technol.* **2010**, *44*, 1875–1880. [[CrossRef](#)] [[PubMed](#)]
30. Oonnittan, A.; Sillanpaa, M.E.T. Water treatment by electro-Fenton process. *Curr. Org. Chem.* **2012**, *16*, 2060–2072. [[CrossRef](#)]
31. Kim, H.J.; Hyun, M.S.; Chang, I.S.; Kim, B.H. A microbial fuel cell type lactate biosensor using a metal-reducing bacterium, *Shewanella putrefaciens*. *J. Microbiol. Biotechnol.* **1999**, *9*, 365–367.
32. Diels, A.M.; Callewaert, L.; Wuytack, E.Y.; Masschalck, B.; Michiels, C.W. Inactivation of *Escherichia coli* by high-pressure homogenisation is influenced by fluid viscosity but not by water activity and product composition. *Int. J. Food Microbiol.* **2005**, *101*, 281–291. [[CrossRef](#)] [[PubMed](#)]
33. Chen, H.S.; Zou, X.G. Treatment in Water Bodies Pollution by Ecological Floating Bed Technology. *China Water Resources* **2005**, *5*, 022.
34. Toyoda, M.; Inagaki, M. Heavy oil sorption using exfoliated graphite: New application of exfoliated graphite to protect heavy oil pollution. *Carbon* **2000**, *38*, 199–210. [[CrossRef](#)]
35. Blumer, M. Oil pollution of the ocean. In *Oil on the Sea*; Springer: Berlin, Germany, 1969; pp. 5–13.
36. Nelson-Smith, A. The problem of oil pollution of the sea. In *Advances in Marine Biology*; Elsevier: Amsterdam, The Netherlands, 1971; Volume 8, pp. 215–306.
37. Molognoni, D.; Chiarolla, S.; Ceconet, D.; Callegari, A.; Capodaglio, A.G. Industrial wastewater treatment with a bioelectrochemical process: Assessment of depuration efficiency and energy production. *Water Sci. Technol.* **2018**, *77*, 134–144. [[CrossRef](#)] [[PubMed](#)]
38. Marashi, S.; Kariminia, H. Performance of a single chamber microbial fuel cell at different organic loads and pH values using purified terephthalic acid wastewater. *J. Environ. Health Sci. Eng.* **2015**, *13*, 27. [[CrossRef](#)] [[PubMed](#)]
39. Kim, K.-Y.; Yang, W.; Ye, Y.; LaBarge, N.; Logan, B.E. Performance of anaerobic fluidized membrane bioreactors using effluents of microbial fuel cells treating domestic wastewater. *Bioresour. Technol.* **2016**, *208*, 58–63. [[CrossRef](#)] [[PubMed](#)]
40. Fujishima, A.; Honda, K. Electrochemical photolysis of water at a semiconductor electrode. *Nature* **1972**, *238*, 37–38. [[CrossRef](#)] [[PubMed](#)]

41. Xu, N.; Zhang, Y.; Tao, H.; Zhou, S.; Zeng, Y. Bio-electro-Fenton system for enhanced estrogens degradation. *Bioresour. Technol.* **2013**, *138*, 136–140. [[CrossRef](#)] [[PubMed](#)]
42. Jadhav, G.; Ghangrekar, M. Performance of microbial fuel cell subjected to variation in pH, temperature, external load and substrate concentration. *Bioresour. Technol.* **2009**, *100*, 717–723. [[CrossRef](#)] [[PubMed](#)]
43. Adani, F.; Baido, D.; Calcaterra, E.; Genevini, P. The influence of biomass temperature on biostabilization–biodrying of municipal solid waste. *Bioresour. Technol.* **2002**, *83*, 173–179. [[CrossRef](#)]
44. Liang, C.; Das, K.; McClendon, R. The influence of temperature and moisture contents regimes on the aerobic microbial activity of a biosolids composting blend. *Bioresour. Technol.* **2003**, *86*, 131–137. [[CrossRef](#)]
45. Wang, Y.; Li, B.; Zeng, L.; Cui, D.; Xiang, X.; Li, W. Polyaniline/mesoporous tungsten trioxide composite as anode electrocatalyst for high-performance microbial fuel cells. *Biosens. Bioelectron.* **2013**, *41*, 582–588. [[CrossRef](#)] [[PubMed](#)]
46. Wang, Z.; Zheng, Y.; Xiao, Y.; Wu, S.; Wu, Y.; Yang, Z.; Zhao, F. Analysis of oxygen reduction and microbial community of air-diffusion biocathode in microbial fuel cells. *Bioresour. Technol.* **2013**, *144*, 74–79. [[CrossRef](#)] [[PubMed](#)]
47. Chakrabarti, S.; Dutta, B.K. Photocatalytic degradation of model textile dyes in wastewater using ZnO as semiconductor catalyst. *J. Hazard. Mater.* **2004**, *112*, 269–278. [[CrossRef](#)] [[PubMed](#)]
48. Smejkal, Q.; Linke, D.; Bentrup, U.; Pohl, M.-M.; Berndt, H.; Baerns, M.; Brückner, A. Combining accelerated activity tests and catalyst characterization: A time-saving way to study the deactivation of vinylacetate catalysts. *Appl. Catal. A Gen.* **2004**, *268*, 67–76. [[CrossRef](#)]
49. Pignatello, J.J.; Oliveros, E.; MacKay, A. Advanced oxidation processes for organic contaminant destruction based on the Fenton reaction and related chemistry. *Crit. Rev. Environ. Sci. Technol.* **2006**, *36*, 1–84. [[CrossRef](#)]
50. Rezaei, F.; Richard, T.L.; Logan, B.E. Analysis of chitin particle size on maximum power generation, power longevity, and Coulombic efficiency in solid–substrate microbial fuel cells. *J. Power Sources* **2009**, *192*, 304–309. [[CrossRef](#)]
51. Xiao, L.; Damien, J.; Luo, J.; Jang, H.D.; Huang, J.; He, Z. Crumpled graphene particles for microbial fuel cell electrodes. *J. Power Sources* **2012**, *208*, 187–192. [[CrossRef](#)]
52. Fan, Y.; Xu, S.; Schaller, R.; Jiao, J.; Chaplen, F.; Liu, H. Nanoparticle decorated anodes for enhanced current generation in microbial electrochemical cells. *Biosens. Bioelectron.* **2011**, *26*, 1908–1912. [[CrossRef](#)] [[PubMed](#)]

